The Progression of Haze Formation in Rabbit Corneas Following Phototherapeutic Keratectomy

Daniel J. Gibson,[1,2] Sonal S. Tuli,[3] and Gregory S. Schultz[1,4]

[1]Institute of Wound Research, University of Florida, Gainesville, Florida
[2]Department of Biochemistry and Molecular Biology, University of Florida, Gainesville, Florida
[3]Department of Ophthalmology, University of Florida, Gainesville, Florida
[4]Department of Obstetrics and Gynecology, University of Florida, Gainesville, Florida

Correspondence: Daniel J. Gibson, University of Florida, 1600 SW Archer Road, Gainesville, FL 32610-0294; gibsondj@ufl.edu.

Submitted: March 5, 2013
Accepted: June 15, 2013

Citation: Gibson DJ, Tuli SS, Schultz GS. The progression of haze formation in rabbit corneas following phototherapeutic keratectomy. *Invest Ophthalmol Vis Sci*. 2013;54:4776–4781. DOI:10.1167/iovs.13-11976

Purpose. To determine the topographical location and time course of development of corneal haze in a phototherapeutic keratectomy model using slit lamp examination, macrophotography, quantitative image analysis, and immunofluorescence staining of corneal sections.

Methods. Rabbit corneas were ablated with an excimer laser and were observed and graded for haze via slit lamp, imaged, and graded by macrophotography. Corneal sections were stained for α-smooth muscle actin (α-SMA) and tenascin-C (TNC). The distribution of haze imaged in the macrophotographs and density of α-SMA and TNC staining were compared. A daily image time course of haze formation was generated using macrophotography.

Results. The first signs of corneal haze were apparent shortly after reepithelialization. The haze was distributed as a ring at the wound margin in all cases, while nearly all corneas also had some central islands of haze initiation. With time, the haze spread within the ablated zone and intensified. The pattern of immunofluorescent staining for α-SMA and TNC at the wound margin mirrored the haze distribution, spread, and intensification with time.

Conclusions. The initiation and spread of subepithelial haze begins shortly after reepithelialization. The haze then spreads from the loci of initiation and becomes more dense with time, maturing as early as 14 days after wounding. The improved temporal and spatial resolution provided by these data improve the current model of light-scattering haze formation in wounded corneas, which will improve the design of studies aimed at maintaining corneal clarity following acute injury or surgery.

Keywords: haze, fibrosis, opacification

The biological response to tissue disruption (i.e., wound healing) is an active field of research, which has consequences for every structure of the eye. Of particular interest is the knowledge of how to control or modulate the wound healing process in the cornea subsequent to photorefractive or phototherapeutic ablation of the cornea. The biological response to surface ablation (SA)–based laser surgery in particular can result in the development of subepithelial haze, regression of correction, or the introduction of higher order optical aberrations. While clinicians do currently have some therapeutic options to broadly dampen the biological response,[1] there are known risks to these treatments[2–5] and better, more targeted options are being actively sought.

In order to develop and test safer treatments to reduce the amount of subepithelial haze in wounded corneas, a better understanding of the haze initiation time point and the haze formation timeline are both needed. This is premised on the idea that any efforts aimed at ameliorating the formation of haze need to be based on the processes that take place in the time *before* the haze starts and before it is firmly established. At present, there is evidence that haze formation begins somewhere between 4 and 7 days after wounding in SA corneas, based on the initiation of collagen deposition[6] and the first measured presence of α-SMA positive myofibroblasts[7], respectively. Based on the observed zone of proliferation underlying and surrounding the wound,[7–9] it has been premised that these underlying cells migrate apically, toward the ocular surface, and differentiate into the light-reflecting phenotype. However, this pattern of migration and haze formation have yet to be demonstrated.

To better understand the fibrotic process that gives rise to subepithelial haze, we observed wounded corneas during the time period when haze initiates and its development using macrophotography to record the gross distribution of haze over the entire wound area. Furthermore, we assessed whether the grossly observed distribution of haze was also represented at the cellular level by immunofluorescent staining for known markers of fibrosis and haze.

Materials and Methods

All animals used in experiments reported herein were treated in a manner consistent with the ARVO Statement for the Use of Animals in Ophthalmic and Vision Research, and in protocols that were reviewed and approved by the University of Florida Institutional Animal Care and Use Committee.

Excimer Laser Wounding

Rabbits were anesthetized using inhaled isoflurane and eyes were topically anesthetized using one drop of tetracaine

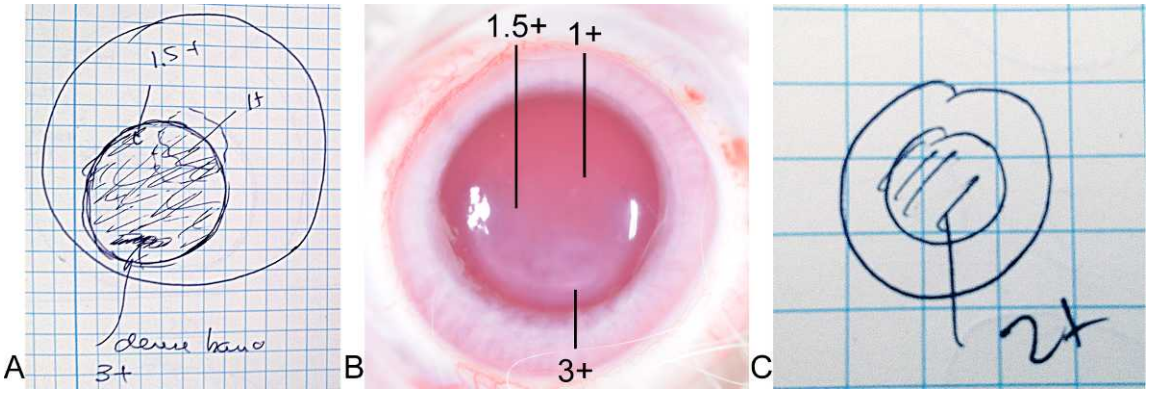

FIGURE 1. A qualitative comparison between slit lamp grading and macrophotography. (**A**) The sketch made by one of the graders of the intensity and distribution of the haze seen in the slit lamp. (**B**) A macrophotograph of the same eye taken after the slit lamp grading. While the heterogeneous distribution of haze in the wound is easily correlated to the sketch in (**A**) and annotations can be easily added to the image, (**C**) not all graders recorded this level of detail.

(Bausch & Lomb, Tampa, FL). Eyes were exposed and the central thickness of the cornea was measured by ultrasonic pachymetry ($n = 5$ central measurements per eye). Each eye then received a central 6.0-mm diameter, 125-μm deep, transepithelial excimer laser phototherapeutic keratectomy (PTK) wound with no transition zone (Nidek EC5000; Nidek, Inc., Freemont, CA). All rabbits received a daily dose of oral meloxicam (0.2 mg/kg; Boehringer Ingelheim, St. Joseph, MO) until wound closure or euthanization.

In Vivo Imaging

Macrophotography. While anesthetized with isoflurane as before, eyes were topically anesthetized with proparacaine HCl (Bausch & Lomb) and pupils were dilated with phenylephrine HCl (Bausch & Lomb) and tropicamide (Bausch & Lomb) eyedrops. Each eye was observed via slit lamp to rule out cataracts prior to imaging the cornea. A digital single lens reflex (dSLR) camera with a macro lens capable of 1:1 reproduction (Tokina 100 mm AT-X M100 AF PRO D; Kenko Tokina Co., Ltd., Tokyo, Japan) and a lens mounted macroflash were then used to obtain the whole wound images. The camera was set to manual exposure with an ISO sensitivity of 100 (for highest quality), an aperture of f/18 (for a useful depth of field), and a shutter speed of 1/250th of a second to obviate both ambient light and camera and subject movement. The flash was set to manual power adjustment and was adjusted until the sclera was highly developed (i.e., bright). Once obtained, this combination of exposure and flash power was used for all images thereafter. For all images, the lens was set to manual focus and prefocused to a 1:1 reproduction ratio. The camera was centered on the visual axis and focused by moving the camera backward and forward until the central cornea was in focus. For the lens used in these experiments, the distance from the subject to the imaging plane is reported to be 11.8 inches, which translates into approximately 4.5 inches between the front of the lens and the subject. However, the subject-to-lens distance will vary depending upon the lens' focal length; accordingly, the necessary flash power for proper exposure will also vary. Each image was checked using the camera's review image screen until a suitably centered and focused image was obtained.

Image Processing. In order to improve the contrast of the native color image, the images were converted to gray scale using only the data in the blue channel (i.e., anti-red). By doing this, the retina is effectively blackened, which enables the finer detail of the scar to be better discerned.

Slit Lamp and Macrophotography Comparison. First, four graders (three clinicians and one experienced researcher) graded five rabbits with bilateral wounds with a slit lamp using a 0 to 4 scale[10] and they were also asked to sketch any details they thought to be important. Next, these same rabbits were imaged using the method above. A slide deck containing the images were emailed to the graders with one natural pair of cornea images per slide. Three separate groups of the same images were present in the slide deck: native color; anti-red gray scale (gray scale); or a combined anti-red gray scale and retina-based normalization where a pixel outside of the wound was used as a reference for black (i.e., zero intensity). The same 0 to 4 scale was used to grade the images. The grades for the four graded sets (one slit lamp and three photo-based) were then analyzed by two methods. First, the scores for each eye were averaged and the variance (standard deviation squared) among the graders' scores for each data set was calculated. A two-tailed Student's *t*-test was used to compare the paired average slit lamp derived scores versus those derived from the photographs. A lack of a statistically significant difference would be interpreted as the techniques being comparable. Next, the reproducibility of the techniques was tested by comparing the average variances in scores among the graders, since lower variance is synonymous with greater reproducibility. Any differences in the observed variances were tested for significance with a two-tailed, pooled *t*-test. A technique with both a lower variance and with statistical significance would indicate that one technique is consistently more reproducible than another. Finally, the scores for each grader were plotted against one another and a linear regression of the relation between the two was plotted. A perfect grader-to-grader correlation would have all of the regressed lines overlapping with a slope equal to 1. The consistency of a method would be qualitatively observable based on how closely the regressed lines overlapped.

Immunohistology

Rabbits were euthanized at several time points during haze formation, and an 8-mm region surrounding the wound was harvested via punch biopsy and was fixed, paraffin embedded, and stained for either α-SMA (A5228, Sigma-Aldrich, St. Louis, MO) or tenascin-C (GW21017, Sigma-Aldrich) using the same conditions for both target proteins as previously described for α-SMA.[11]

RESULTS

Qualitative details of the haze distribution recorded during slit-lamp examination (Fig. 1A) were also apparent in the

TABLE. Statistical Test of the Similarity and Reproducibility of the Techniques

Group	*P* Value of Average Score	*P* Value of Average Variance
Slit lamp vs. native color	0.203	**0.025**
Slit lamp vs. gray scale	0.408	0.056
Slit lamp vs. retinal normalization	0.371	0.162
Native color vs. gray scale	0.723	0.715
Native color vs. retinal normalization	0.250	0.149
Gray scale vs. retinal normalization	0.414	0.360

Bold indicates statistical significance.

macrophotographs (Fig. 1B), although not all graders recorded the slit lamp–observed haze with extensive detail (Fig. 1C). In order to quantitatively compare the two techniques, the Fantes scale[10] of 0 to 4 was used to grade the scars. The average scores of the eyes were statistically compared to determine whether the differences were due to random error ($P > 0.05$) or due to the techniques themselves ($P < 0.05$). The lowest P value obtained was 0.203, indicating that there may be a trend toward a difference in the techniques, but that the difference was not sufficient to consider the scores obtained from the techniques as significantly different. An additional statistical test was also performed to assess how the scores varied (average variance) from grader-to-grader (Table). In all cases, the photographic technique had a lower amount of variance among graders than the slit lamp grading. One photographic technique exceeded statistical significance (slit lamp versus native color, $P = 0.025$), while another was on the threshold of significance (slit lamp versus gray scale, $P = 0.056$). Taken together, these statistical tests indicate that the two techniques are comparable and that the macrophotographic technique is more reproducible than the visual grading performed with a slit lamp. This result can also be qualitatively visualized by the scattered appearance of the linearly regressed grader-to-grader comparisons in Figure 2A versus the near overlapping appearance of those in Figure 2B.

The photographic technique described above was used to record the detailed intensity and distribution of haze as it developed in rabbit corneas in the period following reepithelialization. The first appearance of subepithelial haze became apparent around day 4 or 5 postsurgery, shortly after reepithelialization was complete (Fig. 3). The haze was always distributed as a ring at the wound margin, and sporadically, with another distinct field (Figs. 3A, 3B), or fields (Fig. 3C), of haze in the center of the cornea. With time, the regions of haze appeared to simultaneously become denser, and to "spread" laterally from the regions where they initially appeared (Fig. 4).

Given the greater consistency of occurrence, the haze at the wound margin (i.e., the ring) was the primary focus of the fluorescent micrograph study. The staining for both α-SMA and for TNC began as small light band at the wound margin, which began to become thicker and to spread toward the center of the wound. With time, the thickness of staining in the stroma also increased greatly and in some cases, the entire ablated volume became filled with α-SMA/TNC positive cells leading to a very dense haze (Fig. 5).

The initiation and spread of haze can be viably monitored using macrophotography. Daily images of the same wounded cornea demonstrate the spreading and intensification of haze with time (Fig. 6). If the image pixel intensity of the wound is digitally quantified, a trend to increased average pixel value is seen with time. In this nonoptimized data set, the day-to-day integrated density value does not consistently rise due to noise (poor focus, debris). However, the noise is surmountable if the data is compared on an every-other-day basis, meaning that the viable haze monitoring technique can currently resolve a change in haze equivalent to the amount of light reflecting density that develops in a 48-hour period.

DISCUSSION

In the data presented herein, we've demonstrated that a photograph can be used to grade corneal haze as a substitute to the use of a slit lamp for scar observation and grading purposes—provided that the eye in question has had cataracts ruled out by slit lamp examination. While we do have access to both clinical slit lamps and an in-vivo confocal microscope, obtaining an image of the entire wound is difficult (slit lamp) if not impossible (confocal microscope). Ultimately, we believe that all three imaging techniques are complementary, with the macrophotography providing good overall coverage, the slit lamp ensuring that there is no contribution to the imaged scar by a cataract, and the confocal microscope as the ultimate means to qualify the light reflecting entities (cells versus matrix). Our initial attempt at using photographs to quantify haze in Figure 6 demonstrates that the haze can be quantified, and that the haze difference over any 48+ hour interval can be discerned. However, there is still work to be done to ensure the standardization and reproducibility of this approach. Overall, we anticipate that the imaging technique presented here will greatly aid in the investigation of the haze formation process, since it can record the distribution of haze over the entire wound and it can be done viably. Furthermore, this technique can improve the communication of results from

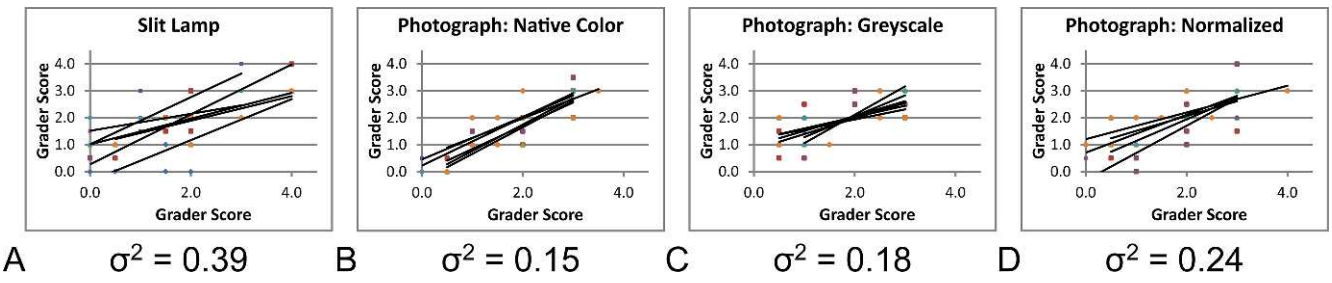

FIGURE 2. A quantitative comparison of slit lamp–based grading and macrophotograph-based grading using the same clinical 0 to 4 scale. Four graders graded five rabbits with bilateral wounds using: (**A**) slit lamp and (**B**–**D**) three sets of digital images with (**B**) no modifications, (**C**) conversion to gray scale, or (**D**) a combined conversion to gray scale and retina-based normalization. The results of statistical tests comparing the techniques and their variances can be found in the Table.

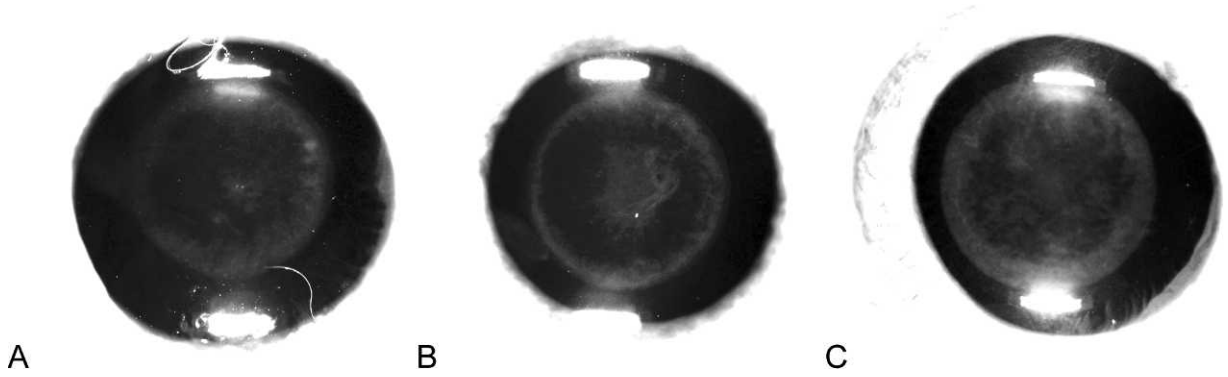

FIGURE 3. Three typical corneal images at day 5 (**A**, **B**) or day 7 (**C**) postwounding. Every wound has a ring of haze at the wound margin and usually some haze initiating in the center, but the pattern is not consistent. (**A**, **B**) Both have what appears to be a single locus of initiation in the center while (**C**) may have several loci.

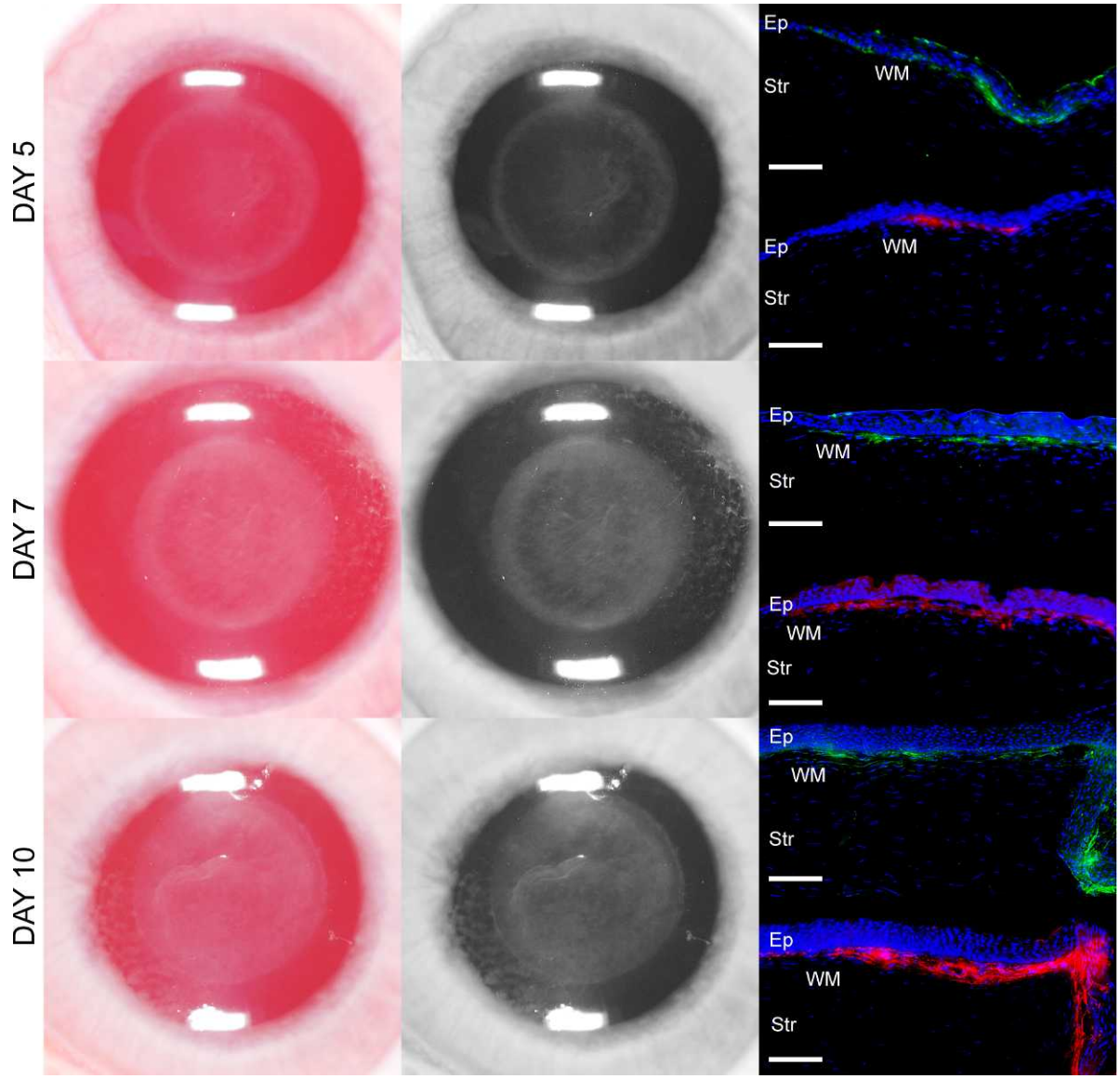

FIGURE 4. The initiation of haze at the wound margin mirrors markers for haze and fibrosis. α-SMA in *green*, TNC in *red*, DAPI in *blue*. Ep, epithelium; Str, stroma; WM, wound margin. The *scale bars* represent 100 μm. In all images taken, the wound margin has a ring of haze while most, but not all also have some initiation of haze in the center. The ring of haze thickens with time and spreads radially inward toward the center of the wound. There are epithelial defects on days 5 and 10 introduced to the cornea when cleaning the surface in preparation for imaging (wrinkled appearance) due to the epithelial instability during this period of wound healing.

Investigative Ophthalmology & Visual Science

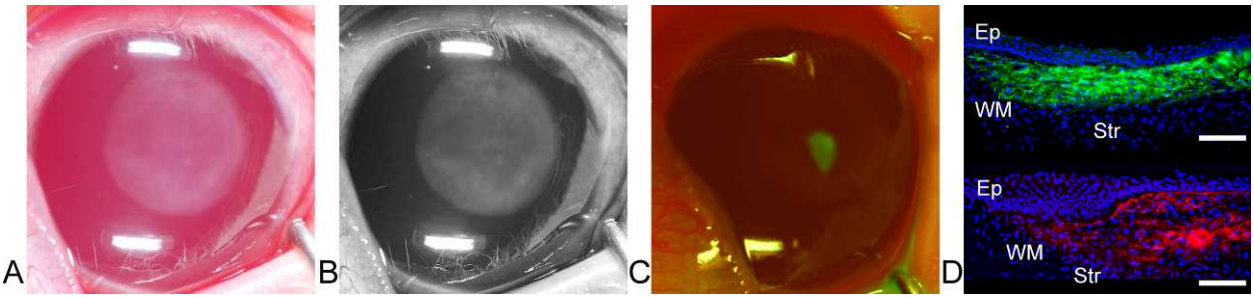

FIGURE 5. The worst scar seen to date seen in a day 14 postwounding cornea. (**A**) True color macrophotograh. (**B**) An anti-red gray scale conversion using only the blue channel to cancel out the red retinal reflex. Note that the relative central clearness is due to (**C**) an epithelial defect (i.e., is fluorescein positive). (**D**) As before, α-SMA in *green*, TNC in *red*, DAPI in *blue*. The *scale bars* represent 100 μm.

trials of antifibrotic agents, where the appearance of the scars can be compared side-by-side for the field as a whole to judge.

The first biological finding using this new approach was that the subepithelial haze begins at two distinct regions within the cornea: a ring at the peripheral wound margin, and as a spot or spots in the wound body. A noted difference in the two regions is that the initiation of haze at the wound margin is consistent while the initiation of haze in the central cornea (arguably more important in terms of visual impact) inconsistently presented with one or more loci of haze initiating in various inconsistent locations (Figs. 3A, 3B vs. 3C). This inconsistency made the study of the central initiation more challenging, and we are actively developing a method to investigate the process in the center of the cornea. We currently hypothesize that our previously reported findings of stromal invasion by the epithelium[11] might be driving the central haze formation process due to the stochastic nature of the invasion process and the apparent randomness of the site and number of haze initiation loci in the wound bed. This hypothesis is granted further plausibility due to the observations of what occurs when epithelial cells are surgically implanted in the center of corneas with LASIK flaps.[12] Additional experiments seeking to observe colocalization of ectopic epithelia within these central regions and migrating myofibroblasts remain to be designed and executed.

The haze at the wound margin was consistently present starting at around day 4, and the distribution and density of the haze appear to comport well with the pattern and density of both the α-SMA and TNC staining. This time point is well correlated with the observed appearance of new collagen,[6] and is reasonable given that myofibroblasts are the known source of said collagen. These results do not contradict previous findings on the appearance of α-SMA positive cells,[7] but do provide evidence of a slightly earlier initiation than 7 days postwounding. The observed patterns of the apparent "spread" of haze or of α-SMA/TNC staining at the wound interface are difficult to reconcile with the initial hypothesis that the fibroblasts underlying the wound proliferate and then migrate apically. It appears that there is an initial migration into the peripheral wound margin, and the spread and intensification are then presumably due to proliferation and lateral or apical migration, respectively. These findings confirm both the roles of migration and proliferation in the formation of haze, though they refine the context and timeline of when and where these processes occur.

Our initial observation of the timing and spreading pattern of haze formation—paired with the observation that the α-SMA positive cells in our experiments, or the unlabeled collagen observed by others[6]—that occupy the region once occupied by the epithelium, led us to an impromptu hypothesis that the epithelium might be contributing to the scar tissue via epithelial-to-mesenchymal transition (EMT). This in turn led us to include TNC staining, given its claimed status as a marker for EMT.[13] Given our observations herein, and our previously reported results from an epithelial cell tracing experiment[11], the use of TNC as a marker for EMT is not supported for use in the cornea. However, given that TNC staining is tightly confined to the stromal α-SMA positive cells, while the α-SMA stains both stromal and epithelial cells, TNC may prove to be a better marker for the myofibroblasts than α-SMA.

The data reported herein support the use of macrophotographs to document and compare corneas presenting with corneal haze. Observations made with this new technique have led us to a refined cellular model of haze formation with two geographically distinct loci of haze initiation, one at the wound margin (ring of haze) and the other frequently initiating a central zone of haze. The migration of myofibroblasts into the wound bed may occur by one of two methods. First, by a slight modification of the initial hypothesis, the cells immediately underlying the apoptotic zone could migrate into the wound at different times, with the peripheral cells migrating first, and the more central cells entering the wound in later waves of migration. Alternatively, cells at the peripheral wound margin, migrate into the wound interface and then "spread" laterally

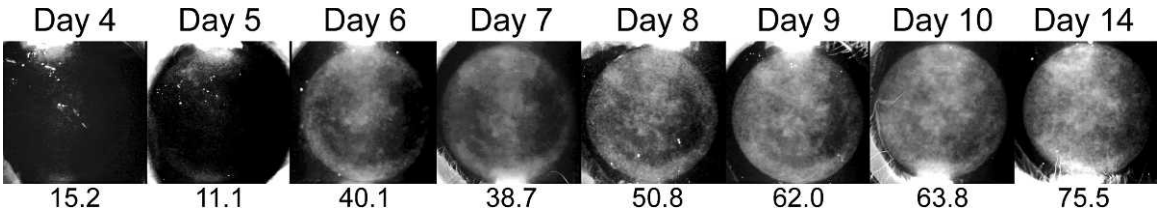

FIGURE 6. A set of images taken of the same wound as the scar develops. The haze begins as a ring at the wound margin and a region in the center. The haze then "spreads" from these loci of initiation to eventually cover the wound, nearing full coverage by day 14. The numbers below represent the mean pixel value of a 6.0-mm scoring region centered on the wound. Note that poor focus (day 7) can cause errors.

into the wound bed, and become more dense ("stack") presumably by a process of proliferation and epithelial displacement. Given that the α-SMA staining and TNC staining are limited to the wound interface, without any positively stained cells deeper in the stroma at the forefront of the staining (Fig. 4, day 5), we believe that the second model is better supported at present. As for the distinct haze in the central regions, we have a hypothetical model supported by previously published data, but which is the subject of an ongoing study. In this model, a portion of epithelium ectopically implants in the central stromal wound bed. The cells nearby and underlying the implant migrate to the implant and form another region of haze initiation. The spread from this point could be presumed to occur by one of the two hypothetical methods described for the wound margin. Ultimately, the dichotomy of margin-initiated versus central body-initiated haze may reconcile conflicting reports of drug efficacy, or explain residual haze not addressed by some therapies. It may also indicate the need for a multifactorial therapeutic approach to address both processes.

In summary, results of these in vivo experiments demonstrate the suitability of using macrophotographs to grossly observe the initiation, spread, and intensification of haze and to quantify the development of corneal haze. The data indicate that fibrosis starts at approximately 1 day after reepithelialization, and the haze continues to spread and become more dense from the initial loci. Immunohistochemical staining of corneas developing haze also provides evidence that the use of tenascin-C is not an absolute marker of EMT, but that it does indicate that it is a potential improvement over the use of α-SMA as a definitive marker for myofibroblasts. Importantly, a relatively simple and straightforward method employing digital macrophotography was developed and validated to document the process of haze formation, in vivo, in a manner consistent both with slit lamp examination and with ex vivo observation of molecular evidence of light reflecting myofibroblasts. Finally, a new cellular model for the initiation and spread of haze was developed, which may be used to generate novel, critically timed, and spatially targeted antifibrotic treatment regimens.

Acknowledgments

Supported by R01 Regulation of Stromal Wound Healing (R01-EY05587); NEI T32 Vision Training Grant (T32-EY007132); NEI Vision Core (EY021721); and supported in part by an unrestricted grant from Research to Prevent Blindness.

Disclosure: **D.J. Gibson**, None; **S.S. Tuli**, None; **G.S. Schultz**, None

References

1. Lane HA, Swale JA, Majmudar PA. Prophylactic use of mitomycin-C in the management of a buttonholed LASIK flap. *J Cataract Refract Surg*. 2003;29:390–392.
2. Roh DS, Funderburgh JL. Impact on the corneal endothelium of mitomycin C during photorefractive keratectomy. *J Refract Surg*. 2009;25:894–897.
3. Kopp ED, Seregard S. Epiphora as a side effect of topical mitomycin C. *Br J Ophthalmol*. 2004;88:1422–1424.
4. Coppens G, Maudgal P. Corneal complications of intraoperative Mitomycin C in glaucoma surgery. *Bull Soc Belge Ophtalmol*. 2010;19–23.
5. Zhivov A, Beck R, Guthoff RF. Corneal and conjunctival findings after mitomycin C application in pterygium surgery: an in-vivo confocal microscopy study. *Acta Ophthalmol*. 2009; 87:166–172.
6. Tuft SJ, Zabel RW, Marshall J. Corneal repair following keratectomy. A comparison between conventional surgery and laser photoablation. *Invest Ophthalmol Vis Sci*. 1989;30: 1769–1777.
7. Mohan RR, Hutcheon AE, Choi R, et al. Apoptosis, necrosis, proliferation, and myofibroblast generation in the stroma following LASIK and PRK. *Exp Eye Res*. 2003;76:71–87.
8. Netto MV, Mohan RR, Ambrosio R Jr, Hutcheon AE, Zieske JD, Wilson SE. Wound healing in the cornea: a review of refractive surgery complications and new prospects for therapy. *Cornea*. 2005;24:509–522.
9. Zieske JD, Guimaraes SR, Hutcheon AE. Kinetics of keratocyte proliferation in response to epithelial debridement. *Exp Eye Res*. 2001;72:33–39.
10. Fantes FE, Hanna KD, Waring GO III, Pouliquen Y, Thompson KP, Savoldelli M. Wound healing after excimer laser keratomileusis (photorefractive keratectomy) in monkeys. *Arch Ophthalmol*. 1990;108:665–675.
11. Gibson DJ, Schultz GS. Ectopic epithelial implants following surface ablation of the cornea. *Invest Ophthalmol Vis Sci*. 2012;53:7760–7765.
12. Wilson SE, Mohan RR, Hutcheon AE, et al. Effect of ectopic epithelial tissue within the stroma on keratocyte apoptosis, mitosis, and myofibroblast transformation. *Exp Eye Res*. 2003; 76:193–201.
13. Dandachi N, Hauser-Kronberger C, More E, et al. Co-expression of tenascin-C and vimentin in human breast cancer cells indicates phenotypic transdifferentiation during tumour progression: correlation with histopathological parameters, hormone receptors, and oncoproteins. *J Pathol*. 2001;193: 181–189.

Investigative Ophthalmology & Visual Science